Polymer 51 (2010) 4784–4789

Contents lists available at ScienceDirect

Polymer

journal homepage: www.elsevier.com/locate/polymer

Partial deuteration probing structural changes in supercontracted spider silk

Roxana Ene, Periklis Papadopoulos*, Friedrich Kremer

University of Leipzig, Institute for Experimental Physics I, Linnéstr. 5, 04109 Leipzig, Germany

ARTICLE INFO

Article history:
Received 2 June 2010
Received in revised form
10 August 2010
Accepted 27 August 2010
Available online 6 September 2010

Keywords:
Spider silk
FTIR
Mechanical

ABSTRACT

Polarized IR-spectroscopic and mechanical measurements are combined to analyse the conformational changes in hydrogenated and partially deuterated major ampullate spider silk of *Nephila edulis*. Special attention is given to supercontraction and to the case where the latter is hindered by mechanical constraints. The determination of the molecular order parameters of the different moieties proves that the amide hydrogen exchange is a selective process, taking place at the surface of β-sheet nanocrystals, implying that these regions are accessible by water. The mechanical properties are changing dramatically when the fiber is wet ("supercontraction") due to the fact that the pre-stress of the chains interconnecting the nanocrystals is irreversibly released. In course of this a novel network of H-bonds is formed, a process which can be suppressed if supercontraction is hindered.

1. Introduction

Dragline silk is produced in the major ampullate spider gland and exhibits the highest toughness among natural and artificial fibers [1]. Due to its high modulus and yield stress [2], it is the most studied silk type [3] becoming in this way the basis of a new family of protein based materials produced through genetic engineering. Research, therefore, is focused on the production of artificial fibers that resemble natural spider silk [4–7]. Despite intense efforts, the properties of manufactured fibers are considerably inferior to the natural one. A better understanding of the structure of spider silk is essential for the design of artificial fibers [6,8–10].

Numerous experimental techniques have been employed for the study of natural and regenerated spider silk, namely X-ray scattering [11–13], nuclear magnetic resonance (NMR) [14,15], Raman [16,17] and infrared spectroscopy [16,18]. Although there is agreement that spider silk is composed of hard, crystalline segments, which are rich in alanine β-sheets, and soft amorphous regions, the structural organization in the amorphous phase is not well understood. Recent studies prove the existence of oriented and non-oriented amorphous phases [11,19], suggesting a three-phase model of spider silk where the amorphous part is composed of soft and hard regions [20]. NMR measurements [21], as well as atomistic simulations [22], show that the amorphous regions are composed of β-turns, 3_1-helices and random structures. The elastic modulus and toughness of the alanine nanocrystals is dependent on their size, with smaller crystals giving rise to better macroscopic mechanical properties [23–25].

In a recent publication we have shown that the amorphous chains in native silk fibers assume conformations far from equilibrium, having high pre-strain. The mechanical properties of spider silk depend on the distribution of pre-strain [26,27]. A direct proof of the existence of high pre-stress applied on the nanocrystals, in the order of hundreds of MPa, is the shrinking by humidity, known as "supercontraction" [26,28]. The effect has been related to the macroscopic mechanical properties such as modulus and strain at break [29]. A three-component combined model of crystals in serial arrangement with amorphous chains and a fraction of chains bypassing them can describe both native and supercontracted states of spider silk [30]. The reduction of sample length is accompanied by the formation of a new network of hydrogen bonds and a minimal decrease in the order parameter of the crystals.

Despite the abundance of studies on the mechanical properties of silk, a detailed knowledge of the way they are modified by water is still missing. Previous studies of hydrated and supercontracted samples have shown that water affects primarily the amorphous parts that do not contain alanine [31–33], but they were not combined with mechanical measurements. For this reason, water permeability of the various moieties in dragline silk and the effect of external strain on them are studied herein by means of hydrogen–deuterium exchange in liquid D_2O. Using aminoacid-specific infrared absorption bands [34–36], deuteration probes the molecular moieties that are accessible by water. The results show

* Corresponding author. Tel.: +49 341 97 32557; fax: +49 341 97 32599.
E-mail address: papadopoulos@physik.uni-leipzig.de (P. Papadopoulos).

0032-3861/$ – see front matter © 2010 Elsevier Ltd. All rights reserved.
doi:10.1016/j.polymer.2010.08.061

that the chemical exchange of amide hydrogen occurs primarily in highly ordered regions, including β-sheeted alanine, suggesting that also the crystalline regions are accessible to water. In addition, the dependence of the order parameter and the microscopic stress on external strain reveals how these moieties are interconnected. This way it is proven that the strong dependence of silk mechanical properties on hydration is due to the conformational changes that take place selectively in the chains with high pre-strain.

2. Experimental

2.1. Sample preparation

The samples used are major ampullate silk from *Nephila edulis* spiders, obtained by forced milking, following a similar procedure to previous works [37]. The silk fiber is double (from the two major ampullate glands) and 400 turns are wound around two metal rods in order to form a dense 6 mm-long layer grid. The constant observation of the gland during milking under a microscope ensures that the sample is not contaminated with other silk types, i.e. minor ampullate or pyriform (SEM images also show only one type of fiber). The native sample is finally glued on the metal rods. Fiber thickness is measured with a Dektak 3030 profilometer and it is found to vary in the range 2–3 μm between the samples, by no more than 10% in the same sample.

Supercontraction with heavy water is accompanied not only by conformational changes, but also by partial amide hydrogen exchange. In order to distinguish between both effects, we study three types of samples (i) a "native" sample (ii) a deuterated supercontracted sample obtained by immersing native silk in D_2O and being allowed to shrink to the maximum possible extent and (iii) a sample with "hindered" supercontraction, prepared by fixing the holder while the sample is immersed in D_2O. The results are compared to previously studied supercontracted silk in H_2O (from the same spider) [30]. All samples are kept in liquid water for 1 h at room temperature; measurements of samples with deuteration times up to 24 h (not shown) show that amide hydrogen exchange does not increase by more than 10% after 1 h. In addition, neutron scattering studies on H/D exchange in spider silk suggest that deuteration rate decreases exponentially with a characteristic time of ~16 min [33]. Afterwards the samples are dried in vacuum at room temperature for 24 h.

Finally, a droplet of parafin oil (for IR spectroscopy, Sigma) is used to wet the samples, in order to decrease the scattering due to the cylindrical geometry of the fibers. The oil has a strong absorption band around 2800–2950 cm^{-1} and a weaker one at ~1450 cm^{-1} and does not affect the rest of the spectrum. Comparison between two identical samples, with and without oil, has shown that it does not deteriorate the mechanical properties, either. In addition, the oil helps maintain a constant deuterium content throughout the measurements, by protecting the sample from humidity. The nearly constant ratio of the intensities of N–H and N–D absorption bands (not shown) proves that this is indeed the case.

2.2. Measurement setup

For the IR measurements a Varian FTIR-Spectrometer equipped with a UMA 500 microscope working in transmission mode is employed. A photovoltaic MCT detector (KMPV50, Kolmar Technologies) working in the range from 750 to 5000 cm^{-1} at a resolution of 1 cm^{-1} is used and a ZnSe grid IR polarizer is inserted in the IR beam so that dichroism can be studied (Fig. 1). The sample is stretched stepwise and rapid-scan measurements under equilibrium (typically 1 h after stretching) are carried out. During IR measurements the force applied to the sample is measured using a sensor (Buster GmbH) capable of measuring up to 10 N. The stress values presented herein refer to the true stress, which is calculated assuming constant volume of the silk fiber [38].

2.3. Data analysis

The bands mentioned in the text are fitted with a sum of Gaussian profiles. A simple straight baseline is subtracted. Simultaneous fits for all polarization directions at a given strain value are made. Transmittance varies sinusoidally with polarization; therefore the absorbance is fitted with the following equation:

$$A(\theta) = -\log_{10}\left(10^{-A_x}\cos^2\theta + 10^{-A_y}\sin^2\theta\right) \quad (1)$$

where A_x and A_y are the absorbance values with light polarized parallel to the x and y axes, respectively, and θ is the polarization angle measured from the x-direction. Assuming cylindrical symmetry around the x-axis the molecular order parameter for vibrations with transition moment parallel to the fiber axis can be defined as:

$$S^{\mathrm{mol}} = \frac{A_x - A_y}{A_x + 2A_y} \quad (2)$$

In order to avoid negative values and allow for direct comparison between parallel and perpendicular vibrations we use a slightly different definition for the perpendicular ones:

$$S^{\mathrm{mol}} = -2\frac{A_x - A_y}{A_x + 2A_y} \quad (3)$$

The molecular order parameter for isotropic samples is equal to zero and becomes 1 for perfect (uniaxial) alignment.

3. Results and disscusion

Major ampullate silk fiber is composed of two high molecular weight proteins, MaSp1 and MaSp2 (Major ampullate spidroin 1 and 2) and the major part of the macromolecules contains four

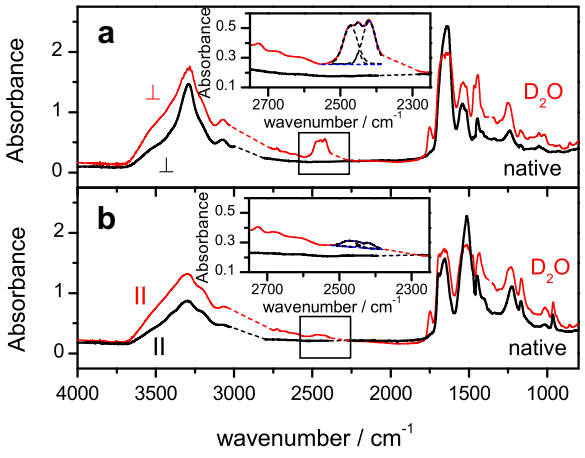

Fig. 1. IR absorption spectra of major ampullate silk from *Nephila edulis* in native (thick black curve) and supercontracted with D_2O state (thin red curve) measured with (a) perpendicular or (b) parallel polarization with respect to the fiber axis. The analysis is focused in the spectral region between 2550 and 2350 cm^{-1} (inset), because it contains the ND stretching bands resulting from the exchange of hydrogen with deuterium. The strong dichroism reflects the high alignment of the moieties accessible to water. The assignments of the bands are summarized in Table 1. Dashed lines represent the positions of the paraffin oil and CO_2 bands (For interpretation of the references to colour in this figure legend, the reader is referred to the web version of this article).

Table 1
List of absorption bands used for the structural analysis of major ampullate spider silk. The molecular assignment and the orientation of the transition moment with respect to the protein backbone are included.

Wavenumber (cm^{-1})	Molecular assignment	Orientation
964	β-PAla (CH_3 rock, NC^{α} stretch)	∥
1015	PGly I (NC^{α} stretch)	∥
1028	PGly II (NC^{α} stretch)	∥
1750	Non H-bonded C=O	⊥
2420	ND-stretching	⊥
2449	ND-stretching	⊥
2478	ND-stretching	⊥

patterns of aminoacids: $(Ala)_n$, AlaGly, GlyGlyX, GlyProGlyXX (X: any aminoacid) [39,40]. The infrared absorption spectra of native and supercontracted with D_2O silk samples (under zero stress) are compared in Fig. 1. Similar to our previous studies [26,30], in both states a high dichroism of the amide bands and the aminoacid-specific bands in the region 1100–900 cm^{-1} is observed [35,41–44]. However, in constrast to silk supercontracted with H_2O [30], the spectrum of the deuterated sample shows notable differences: (a) the amide II band ($\sim$1520 cm^{-1}) becomes double, (b) the spectral region 2550–2350 cm^{-1} (Fig. 1 inlet) contains the ND stretching bands resulting from the exchange of hydrogen with deuterium, (c) the aminoacid-specific bands (1100–900 cm^{-1}) show small, but measurable, frequency shifts and (d) a new absorption band appears at $\sim$1750 cm^{-1}. The appearance of the new component of the amide II band at lower wavenumbers is due to partial deuteration of the silk. The high absorbance in combination with the cylindrical sample geometry, as well as the overlapping with other bands, preclude a quantitative analysis, so this band will not be discussed further. The other ones, however, can give detailed information about the effect of water on the different molecular moieties. The absorption bands that are discussed below are summarized in Table 1.

Before the discussion of the effects on the microscopic structure, it is important to verify that the mechanical properties of silk samples supercontracted in H_2O and D_2O are the same. The sample made by "hindered" supercontraction, has similar mechanical properties to the native state, because pre-strain is not released. In contrast, silk supercontracts by $\sim$40–50% in both H_2O and D_2O. The exact amount depends on the pre-strain of the amorphous chains and varies slightly even for samples from the same spider obtained on different days. The stress–strain curve of the deuterated supercontracted silk (Fig. 2) exhibits three regimes, similar to the previously published detailed results on silk supercontracted in H_2O [26,30]; an initial stiff one at low strain, a plateau and finally an increase of the modulus. The initial stiff state has been attributed to the formation of a new hydrogen bond network during supercontraction, which breaks irreversibly, when stress exceeds $\sim$0.2 GPa [30]. The plateau is due to the nearly zero pre-strain of the amorphous chains in supercontracted silk, which respond like loose worm-like chains. At higher strain, the amorphous parts are stretched and the modulus increases, as expected. This stress–-strain curves have been reproduced by mean-field models [26] and are in good agreement with recent results of simulations on alanine nanocrystals in serial arrangement with amorphous chains [24]. The simulations do not take pre-strain into account (which is nearly zero in supercontracted silk) and also also predict three regimes; an initial breaking of H-bonds in semiamorphous domains, an unraveling of protein chains and a final stiff regime.

The molecular order of the various moieties (Fig. 3) can be determined from the polarization-dependent measurements. In native silk the molecular order parameter S^{mol} of crystals is constant at $\sim$0.9, showing that spinning orients the alanine-rich nanocrystals almost perfectly. Supercontraction with D_2O (or H_2O [26,30]) only slightly decreases the order of crystals, suggesting that the effect cannot be attributed to crystal reorientation, but rather to release of pre-strain, i.e. reduction of the amorphous chain end-to-end length. The nanocrystal order parameter increases during stretching, but reaches the value of native silk well before reaching the original length (zero strain). On the other hand, the S^{mol} values of the low persistence length PGly I and II that constitue the major part of the amorphous chains are significantly lower, but the non-zero value and the slightly increase with stress also imply that these chains are pre-strained [29].

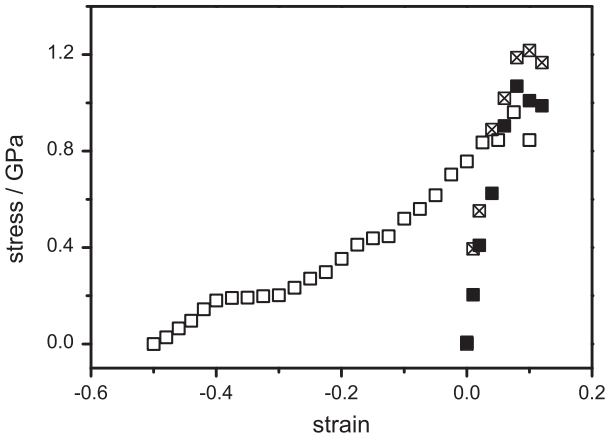

Fig. 2. Stress versus strain for *Nephila edulis* major ampullate silk in different states: native (cross symbols), hindered supercontraction (full symbols) and supercontracted in D_2O (empty symbols). Strain is calculated with respect to the native sample length. The respective curves for samples supercontracted in H_2O have been published previously [30]. The error bars are smaller than the symbol size.

As seen already in Fig. 1, the dichroism of the N–D band is higher than that of the N–H, for all three Gaussian components of this band (Fig. 3). This result, in combination with the fact that the integrated absorbance of the ND band amounts to only a few percent of the NH band, implies that the hydrogen–deuterium exchange is a highly selective process [45]. The results suggest that

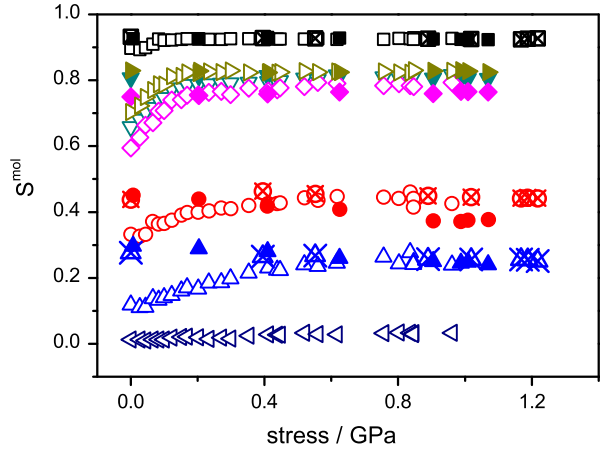

Fig. 3. Molecular order parameter S^{mol} as a function of macroscopic stress. Native (cross symbols), hindered (full symbols) and supercontracted silk in D_2O (empty symbols) are compared. The symbols represent the band (squares: 964 cm^{-1}, circles: 1015 cm^{-1}, up triangles: 1028 cm^{-1}, left triangles: 1750 cm^{-1}, right triangles: 2420 cm^{-1}, down triangles: 2449 cm^{-1}, rhombuses: 2478 cm^{-1}, see Table 1). In all states the alanine-rich structures are highly oriented, while the glycine-rich amorphous chains exhibit lower order. The ND bands resulting from sample deuteration are also highly oriented, while the C=O band shows a low molecular order. The error bars are smaller than the symbol size.

the chemical exchange of amide hydrogen occurs in highly ordered moieties including β-sheeted alanine residues and amorphous chains with high pre-strain. It is known that H–D exchange is faster in unfolded structures [46,47] and may not take place at all in residues "hidden" by protein folding and inaccessible to water [48]. The perpendicular orientation of the respective average transition moments (Fig. 1) proves that the helical structures, where the N–H bonds are preferably oriented parallel to the fiber axis, are not affected. These findings are consistent with neutron scattering experiments that suggest the selective N-deuteration of polyglycine with short-range order [33]. The stress dependence of S^{mol} shows two regimes; at low stress the order increases rapidly, until a threshold of ~0.2 GPa is exceeded, after which the order remains constant. This threshold corresponds to the end of the initial stiff regime in the stress–strain dependence (Fig. 2) [30] and shows that the highly ordered molecular pre-strain chains, that are accessible to water, control the mechanical properties. It is notable that the two polyglycine bands, corresponding to amorphous chains, reach the maximum order at higher stress.

Previous studies have shown that the frequency of main chain vibrations, such as β-sheet polyalanine, varies linearly with crystal stress and can be used as a force probe on a molecular level [37]. The comparison of the macroscopic and crystal stress can reveal the interconnection between phases for both native and supercontracted silk (Fig. 4). The linear thresholdless dependence of the crystal band shift on stress in case of native and hindered supercontracted state suggests that the alanine-rich β-sheeted crystals and the amorphous phase are in a primarily serial arrangement. The equal slope in both cases, as well as the similar mechanical properties (Fig. 2) indicate that the nanostructure and pre-stress have not changed. However, the partially deuterated sample made by hindered supercontraction exhibits lower vibration frequencies by ~1.5 cm^{-1}. Since this difference cannot be attributed to different crystal stress, it is a proof that the polyalanine nanocrystals are deuterated to a small extent, which could not be detected by neutron scattering experiments [33]. For comparison, this vibration in fully N-deuterated polyalanine is shifted to 942 cm^{-1} [35]. The much smaller shift in the present case suggests that most likely only the surface of the nanocrystals is accessible by water, in agreement with recent NMR studies [31,49].

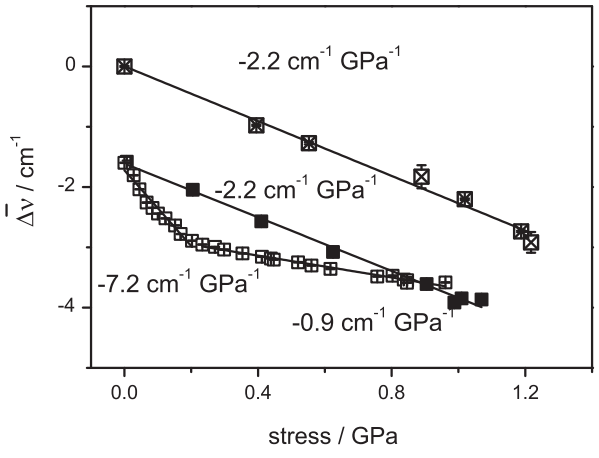

Fig. 4. Microscopic effects of stress. The polyalanine-crystal absorption band at 964 cm^{-1} exhibits a shift $\Delta\bar{\nu}$ to lower wavenumbers in response to external mechanical stress. A linear frequency dependence on stress is observed in the native (cross symbols) and hindered state (full symbols), showing that alanine-rich β-sheeted crystals and the amorphous phase are in a primarily serial arrangement. In contrast, the band shift dependence on stress for the supercontracted with D_2O sample (empty symbols) shows two regimes. The limit between the two regimes also corresponds to a transition from the linear stress–strain dependence to the stress plateau (Fig. 2). The error bars are smaller than the symbol size, if not indicated otherwise.

The band shift dependence on stress for the supercontracted with D_2O (or H_2O [30]) sample is different. First, the band shift at zero stress is almost the same as in the "hindered" sample. Due to the fact that pre-stress is completely released after supercontraction, one would expect a higher frequency. This observation shows that supercontraction makes the amorphous phase more permeable due to conformational changes, allowing more water molecules to reach the surface of the crystals, compared to the case of deuteration with fixed sample length. Second, two regimes are observed, similar to our previous studies [30], instead of a linear dependence. The difference of the stiffness between the chains that directly connect the crystals and the ones that bypass them is reflected in the different $\Delta\bar{\nu}/\sigma$ slopes, according to the previously published model. The stress limit between the two regimes corresponds to the similar observations in the mechanical properties (Fig. 2) and the order parameter of the deuterated moieties (Fig. 3). It is, therefore, concluded, that the amorphous chains that have high pre-strain in the native state form the new, stiff, hydrogen bond network, after supercontraction.

A further major difference between the samples supercontracted in H_2O and D_2O is the band at 1750 cm^{-1} (Fig. 1). This band cannot be assigned to deuterated moieties, since the vibration frequencies are, in general, lower than those of the hydrogenated counterparts. Its proximity with the amide I band implies that it is also a carbonyl stretching vibration, but the higher frequency suggests that the band originates from carbonyls that are not hydrogen-bonded [50]. Such a band is normally not observable in proteins, due to the abundance of protic hydrogen atoms in proteins and in bound water. However, in some special cases, where the formation of hydrogen bonds is not favorable, this band becomes detectable, e.g. in structures containing proline [51] or β-turns [52]. In silk it has, compared to amide I, a relative intensity of 1%, implying that the fraction of non-hydrogen bonded carbonyls is similarly small. Furthermore, the molecular order parameter is close to zero (Fig. 3), proving that these moieties are disordered. The fact that this band is observed only when the sample supercontracts in D_2O (it is weak after "hindered" supercontraction) suggests that the effect is related to changes of hydrogen bonding in the deuterated main chain. The reason for this might be caused by the slightly different strength of the deuterium bond compared to the hydrogen bond. This idea is depicted in Fig. 5. Water breaks the hydrogen bond network in the amorphous phase, but after supercontraction and drying of the sample, not all aminoacid residues are in conformations that favor the formation of hydrogen bonds, especially interchain ones, such as in β-sheets. In these cases the system must overcome the barrier for the reorientation of the main chains, as well as the deformation of the peptide bonds. In order for the hydrogen (or deuterium) bond to form, the respective enthalpy must be higher than these energy costs. The energies of the hydrogen- and deuterium-bonded states in Fig. 5 are, respectively,

$$E_H = E_0 + E_C - E_{OH} \quad (4)$$

$$E_D = E_0 + E_C - E_{OD} \quad (5)$$

where E_{OH} and E_{OD} represent the energy needed for the formation of the H/D-bonds, E_0 is the energy of the non-bonded state and E_C the energy required for the conformational changes. Assuming that no secondary effects take place, one should expect that the ratio of non-bonded carbonyls in deuterated and protonated samples would be $\exp((E_H - E_D)/k_BT)$, with k_BT ~2.5 kJ mol^{-1} at room temperature. Unfortunately the difference of hydrogen- and deuterium-bond enthalpies is not well known. Deuteration is commonly assumed not to affect the structure [53]. However, studies of proteins [54] and, especially, carboxylic acids [55–57]

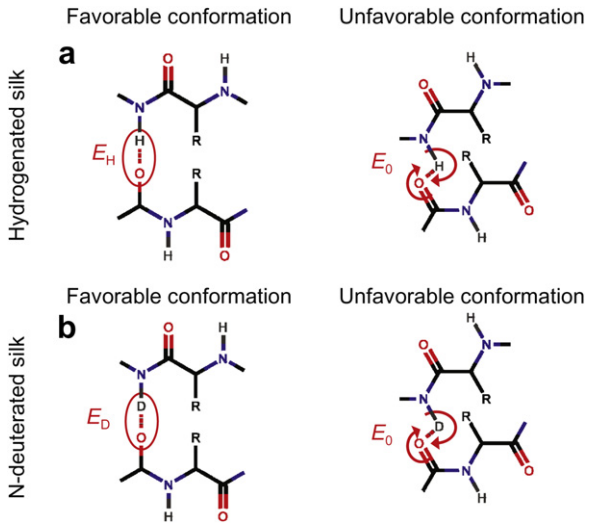

Fig. 5. Mechanism of the formation of (a) hydrogen bonds and (b) deuterium bonds in the amorphous chains of spider silk. During supercontraction the chain conformation changes, so there are roughly two possible conformations, with respect to the ability to form an H- or D-bond: the favorable conformation, where the peptides are aligned, and the unfavorable conformation, where due to supercontraction the peptides are no more aligned and the formation of O···H or O···D (E_0) requires an additional energy for the rotation of the peptide chains. The difference in the enthalpies of hydrogen and deuterium bonds (E_H and E_D, respectively) may prevent the formation of the bond in the latter case, giving rise to the absorption band from free (non-bonded) C═O groups.

show that the deuterium bond is weaker, with E_H–E_D up to 1 kJ mol^{-1}. This is not enough to explain quantitatively the observed difference, but the presented idea is oversimplified and a quantum mechanical treatment is necessary. In any case, it shows that deuteration can induce small changes in protein hydrogen bonding, especially when major conformational changes take place [58,59].

The microscopic and macroscopic effects of hydration that are probed by combined IR and mechanical measurements with or without deuteration are summarized in Fig. 6. Water accesses most easily the residues that are weakly hydrogen bonded, i.e. amorphous chains with high pre-strain and parts of crystal surface. The former become more mobile and tend to reach their equilibrium conformation. When the sample is allowed to shrink, the pre-strain is released, decreasing inter-crystal spacing and ultimately inducing the formation of a new hydrogen-bonded network in the amorphous phase.

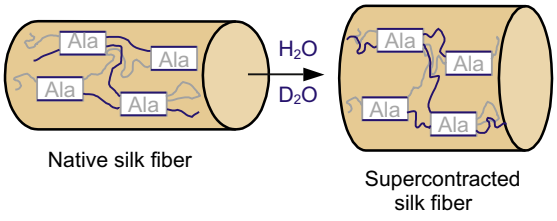

Fig. 6. Accessibility of silk proteins to water. The exchange of amide hydrogens takes place primarily at highly ordered moieties, including amorphous chains with high pre-strain and possibly parts of the alanine nanocrystal surface (marked with blue). The structure of silk remains practically identical after hindered supercontraction, but the spacing between the crystals, as well as pre-strain, decrease, when the fibers are allowed to shrink (For interpretation of the references to colour in this figure legend, the reader is referred to the web version of this article).

4. Conclusions

Using aminoacid-specific infrared absorption bands, deuteration probes the molecular moieties that are accessible by water. The chemical exchange of amide hydrogen with deuterium takes place selectively in highly ordered regions, including the surface of the nanocrystals. The dependence of the order parameter and the microscopic stress on external strain reveals how the moieties are interconnected. This way it is proven that the strong dependence of silk mechanical properties on hydration is due to the conformational changes that take place selectively in the chains with high pre-strain.

Acknowledgements

We thank the Leipzig Graduate School “Building with Molecules and Nano-objects” (BuildMoNa) for financial support and Prof. H. Siesler for fruitful discussions.

References

[1] Lee S, Pippel E, Gösele U, Dresbach C, Qin Y, Chandran CV, et al. Science 2009;324:488–92.
[2] Gosline J, Guerette PA, Ortlepp CS, Savage KN. J Exp Biol 1999;202:3295–303.
[3] Blackledge TA, Swindeman JE, Hayashi CY. J Exp Biol 2005;208:1937–49.
[4] Shao Z, Vollrath F, Yang Y, Thogersen HC. Macromolecules 2003;36:1157–61.
[5] Qiu W, Teng W, Cappello J, Wu X. Biomacromolecules 2009;10(3):602–8.
[6] Hagn F, Eisoldt L, Hardy JG, Vendrely C, Coles M, Scheibel T, et al. Nature 2010;465:239–44.
[7] Hardy JG, Römer LM, Scheibel TR. Polymer 2008;49:4309–27.
[8] Jin H, Kaplan DL. Nature 2003;424:1057–61.
[9] Knight DP, Vollrath F. Naturwissenschaften 2001;88:179–82.
[10] Heim M, Keerl D, Scheibel T. Angew Chem Intl Ed 2009;48:3584–96.
[11] Glišović A, Vehoff T, Davies RJ, Salditt T. Macromolecules 2008;41:390–8.
[12] Miller LC, Putthanarat S, Eby RK, Adams W. Int J Biol Macromol 1999;24:159–65.
[13] Riekel C, Vollrath F. Int J Biol Macromol 2001;29:203–10.
[14] Kümmerlen J, van Beek JD, Vollrath F, Meier BH. Macromolecules 1996;29:2920–8.
[15] van Beek JD, Hess S, Vollrath F, Meier B. Proc Natl Acad Sci U S A 2002;99:10266–71.
[16] Shao J, Zheng J, Liu J, Carr CM. J Appl Polym Sci 2005;96:1999–2004.
[17] Rousseau ME, Lefèvre T, Beaulieu L, Asakura T, Pézolet M. Biomacromolecules 2004;5:2247–57.
[18] Dong Z, Lewis RV, Middaugh CR. Arch Biochem Biophys 1991;284(1):53–7.
[19] Simmons A, Ray E, Jelinski LW. Macromolecules 1994;27:5235–7.
[20] Vollrath F, Porter D. Soft Matter 2006;2:377–85.
[21] Holland GP, Creager MS, Jenkins JE, Lewis RV, Yarger JL. J Am Chem Soc 2008;130:9871–7.
[22] Keten S, Buehler MJ. Appl Phys Lett 2010;96:153701.
[23] Keten S, Xu Z, Ihle B, Buehler MJ. Nat Mater 2010;9:359–67.
[24] Nova A, Keten S, Pugno NM, Redaelli A, Buehler MJ. Nano Lett 2010;10(7):2626–34.
[25] Du N, Liu XY, Narayanan J, Li L, Lim MLM, Liy D. Biophys J 2006;91:4528–35.
[26] Papadopoulos P, Sölter J, Kremer F. Colloid Polym Sci 2009;287:231–6.
[27] Papadopoulos P, Ene R, Weidner I, Kremer F. Macromol Rapid Commun 2009;30:851–7.
[28] Elices M, Pérez-Rigueiro J, Plaza G, Guinea GV. J Appl Polym Sci 2004;92:3537–41.
[29] Liu Y, Shao Z, Vollrath F. Nat Mater 2005;4:901–6.
[30] Ene R, Papadopoulos P, Kremer F. Soft Matter 2009;5:4568–74.
[31] Li X, Eles PT, Michal CA. Biomacromolecules 2009;10:1270–5.
[32] Yang Z, Liivak O, Seidel A, LaVerde G, Zax DB, Jelinski LW. J Am Chem Soc 2000;122:9019–25.
[33] Sapede D, Seydel T, Forsyth VT, Koza MM, Schweins R, Vollrath F, et al. Macromolecules 2005;38:8447–53.
[34] Lee S, Krimm SJ. Raman Spectrosc 1998;29:73–80.
[35] Dwivedi AM, Krimm S. Macromolecules 1982;15:186–93.
[36] Siesler H. Polym Bull 1983;9:557–62.
[37] Papadopoulos P, Sölter J, Kremer F. Eur Phys J E 2007;24:193–9.
[38] Guinea GV, Pérez-Rigueiro J, Plaza GR, Elices M. Biomacromolecules 2006;7:2173–7.
[39] Hayashi CY, Shipley NH, Lewis RV. Int J Biol Macromol 1999;24:271–5.
[40] Gatesy J, Hayashi C, Motriuk D, Woods J, Lewis R. Science 2001;291:2603–5.
[41] Moore WH, Krimm S. Biopolymers 1976;15:2465–83.

[42] Dwivedi AM, Krimm S. Macromolecules 1982;15:177–85.
[43] Dwivedi AM, Krimm S. Biopolymers 1982;21:2377–97.
[44] Moore WH, Krimm S. Biopolymers 1976;15:2439–64.
[45] Kraus M, Janek K, Beinert M, Krause E. Rapid Commun Mass Spectrom 2000;14:1094–104.
[46] Hoofnagle AN, Resing KA, Ahn NG. Annu Rev Biophys Biomol Struct 2003;32:1–25.
[47] Kamerzell TJ, Middaugh CR. Biochemistry 2007;46:9762–73.
[48] Wu Y, Murayama K, Ozaki YJ. Phys Chem B 2001;105:6251–9.
[49] Holland GP, Lewis RV, Yarger JL. J Am Chem Soc 2004;126:5867–72.
[50] Barth A. Prog Biophys Mol Biol 2000;74:141–73.
[51] Martino M, Bavoso A, Guantieri V, Coviello A, Tamburro AJ. Mol Struct 2000;519(1–3):173–89.
[52] Krimm S, Bandekar J. Adv Protein Chem 1986;38:181–364.
[53] Fisher SJ, Helliwell JR. Acta Crystallogr 2008;A64(3):359–67.
[54] Chen C, Liu I, MacColl R, Berns DS. Biopolymers 1983;22(4):1223–33.
[55] Buckingham AD, Fan-Chen L. Int Rev Phys Chem 1981;1(2):253–69.
[56] Marechal Y. Chem Phys Lett 1972;13(3):237–40.
[57] Sauren H, Winkler A, Hess P. Chem Phys Lett 1995;239(4–6):313–9.
[58] Mortensen A, Nielsen OF, Yarwood J, Shelley V. J Phys Chem 1995;99 (13):4435–40.
[59] Pace CN. Nat Struct Mol Biol 2009;16(7):681–2.